

# Dielectric elastomer film actuators: characterization, experiment and analysis\*

Yanju Liu<sup>1,3</sup>, Liwu Liu<sup>1</sup>, Zhen Zhang<sup>2</sup> and Jinsong Leng<sup>2,3</sup>

<sup>1</sup> Department of Astronautical Science and Mechanics, Harbin Institute of Technology (HIT), No 92 West Dazhi Street, PO Box 301, Harbin 150001, People's Republic of China

<sup>2</sup> Centre for Composite Materials, Science Park of Harbin Institute of Technology (HIT), No 2 YiKuang Street, PO Box 3011, Harbin 150080, People's Republic of China

E-mail: [yj\\_liu@hit.edu.cn](mailto:yj_liu@hit.edu.cn) and [lengjs@hit.edu.cn](mailto:lengjs@hit.edu.cn)

Received 9 October 2008, in final form 6 June 2009

Published 17 July 2009

Online at [stacks.iop.org/SMS/18/095024](http://stacks.iop.org/SMS/18/095024)

## Abstract

Silicone is a common dielectric elastomer material. Actuators made from it show excellent activation properties including large strains (up to 380%), high energy densities (up to  $3.4 \text{ J g}^{-1}$ ), high efficiency, high responsive speed, good reliability and durability, etc. When a voltage is applied on the compliant electrodes of the dielectric elastomers, the polymer shrinks along the electric field and expands in the transverse plane. In this paper, a silicone dielectric elastomer is synthesized and the area strains are tested under different electric fields. Pre-strain and a certain driving electric field are applied to the film and the induced large strain by the Maxwell stress is measured. Barium titanate ( $\text{BaTiO}_3$ ) was incorporated into the silicone to fabricate a new dielectric elastomer: the experimental results show that the elastic modulus and dielectric constant were significantly improved. The experimental results coincide well with those of finite element analysis at a large deformation. Also, a theoretical analysis is performed on the coupling effects of the mechanical and electric fields. A nonlinear field theory of deformable dielectrics and hyperelastic theory are adopted to analyze the electromechanical field behavior of these actuators. Also the mechanical behavior of the dielectric elastomer undergoing large free deformation is studied. Finally, the constitutive model of a dielectric elastomer composite under free deformation and restrained deformation is derived.

(Some figures in this article are in colour only in the electronic version)

## 1. Introduction and actuation principle

In the past 10 years, electroactive materials, capable of showing elongation and bending under electric fields, have attracted much attention [1–7]. Among them, ‘piezo-’ and ‘ferro-’ electric materials are less developed due to their poor mechanical performances. In contrast, an electroactive polymer called a dielectric elastomer (DE) has become one of the most promising materials of actuators. This is due to its superb properties: e.g. large recoverable deformation

(up to 380%), high energy density ( $3.4 \text{ J g}^{-1}$ ) and fast response [8–11]. The DE is first proposed and studied in 1991 by SRI International. Later, Jet Propulsion Lab from NASA, Penn State University, ETH Switzerland, etc, started their own research on DE. With its excellent mechanical performance, DE found its applications in such industrial areas where strictly flexibility, small size and high precision are required.

The electroactive effect of the dielectric elastomer depends on three factors: the electrical force between electrodes, the microstructure and the mechanical properties of the material. The electrodes are in fact compliant carbon grease spread uniformly on both surfaces of the DE film [12–17]. When these electrodes are applied with a voltage, the DE film will expand in plane and contract perpendicularly, see figure 1.

\* This article was originally submitted for the special section ‘Smart Composite Materials: Selected Papers from the International Conference on Multifunctional Materials and Structures (MFMS 08) (Hong Kong, 28–31 July 2008)’, Smart Materials and Structures, volume 18, issue 7.

<sup>3</sup> Authors to whom any correspondence should be addressed.

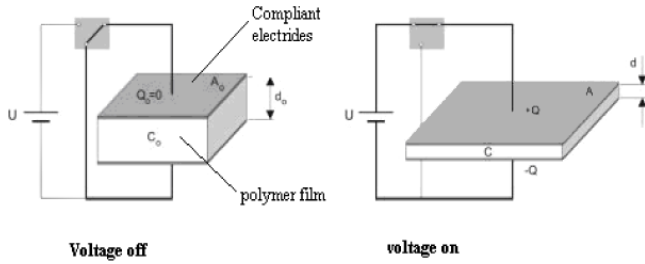


Figure 1. Working mechanism of the dielectric elastomer actuator.

Through this electrostatic model, one can deduce the electrostatic force developed between electrodes. The pressure  $P$  is found to be

$$P = \epsilon_0 \epsilon_r E^2 = \epsilon_0 \epsilon_r \left( \frac{V}{t} \right)^2 \quad (1)$$

where  $\epsilon_0$  and  $\epsilon_r$  denote the dielectric constants of the vacuum and dielectric elastomer, respectively.  $V$  is the electric field strength,  $E$  is the electric field constant and  $t$  represents the thickness of the dielectric film.

In the above equation,  $P$  is generated by the in-plane elongation and the vertical contraction. However, the effect of the in-plane tension is predicted to be very small, and thus neglected. Then the vertical contraction is the only factor to be considered. The pressure induces a corresponding strain along the thickness direction in the DE film, which is nonlinear in the case of large deformation. With the boundary conditions, this strain is found to be

$$\epsilon_z = -\frac{p}{Y} = -\frac{\epsilon_0 \epsilon_r}{Y} E^2 \quad (2)$$

where  $Y$  is the elastic modulus, depending nonlinearly on the strain itself. This is also true for  $\epsilon_r$ . We now introduce a strain ratio  $\Lambda = \epsilon_0 \epsilon_r / Y$ , which reflects the influence of the material's character on strain. Hence one has  $\epsilon_z = -\Lambda E^2$ .

Since the dielectric elastomer is assumed to be incompressible, one immediately has

$$(1 + \epsilon_x)(1 + \epsilon_y)(1 + \epsilon_z) = 1. \quad (3)$$

Introducing the deformation ratio of the total area:

$$S_{\text{area}} = (1 + \epsilon_x)(1 + \epsilon_y) - 1. \quad (4)$$

$$\text{one obtains } (1 + S_{\text{area}})(1 + \epsilon_z) = 1. \quad (5)$$

This shows that  $S_{\text{area}}$  is directly related to the strain along the thickness direction. Measurement of the ratio of area change is relatively precise and easy to perform. The theory of continuum mechanics is employed to define the ratio of area change. In this paper, we treat  $S_{\text{area}}$  as an experimentally measured quantity.

## 2. Synthesis and electroactive deformation test

The silicone dielectric elastomer (BJB TC5005 A-B/C) comprises three components: silicone monomer, also known

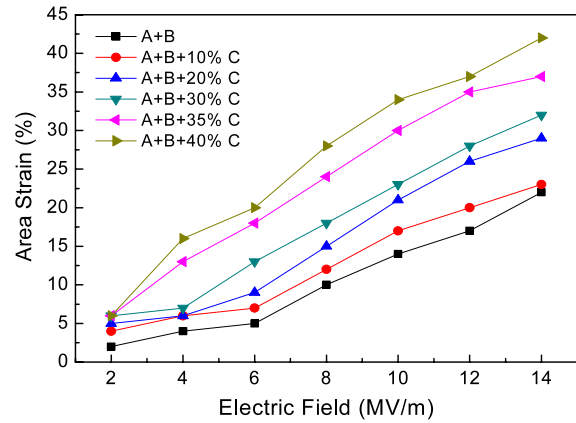


Figure 2. Electric field versus surface strain with different percentages of plasticizer C (pre-strain is 0%).

as silicone glue (A), catalyst (B) and plasticizer (C), where A is mixed proportionally with B and C. The mixture of these components is spread uniformly on a prepared matrix and then a solidification follows, resulting in the silicone elastomer being obtained. Furthermore, with carbon grease painted uniformly on both of its surfaces, a silicone film actuator is then fabricated.

A series of silicone films with different per cents of component C have been developed: A + B, A + B + 10% C, A + B + 20% C, A + B + 30% C, A + B + 35% C and A + B + 40% C. Note especially that the first one A + B has no component C in it and has a ratio of A:B = 10:1.

The silicone film actuators obtained from the matrix with different per cents of plasticizer C all have a size of  $100 \times 100 \times 0.5 \text{ mm}^3$ . The carbon grease is applied around a central circle with a radius of 30 mm. The silicone film actuator is fixed to a special square mold. We performed electrically induced deformation experiments on the silicone film actuator under different pre-stretch rates (0%, 225%, 400%, 625% and 900%). We listed only the two representative stretch rates of 0% and 400% (figures 2 and 3).

The relation between the electric field and the area strain in figures 2 and 3 is given by the following steps:

(1) Calculation of the electric field

For both the pre-stained and un-pre-stained dielectric elastic silicone film with different percentages of C and barium titanate, the electric field is calculated according to the electric field basic formula,  $E = U/d$ , in the condition that the voltage  $U$  and the film thickness is imposed.

(2) Record and calculation of the area strain

In order to calculate the area strain of the working film, the areas of the circular electrode before and after exerting the electric field are firstly captured by a CCD camera with the same modifiable parameters. Then the area strain is calculated by comparing these two areas of the circular electrode. This method is capable of calculating the area strain of different situations, such as films with different percentages of C, with different pre-strain ratios and different contents of barium titanate. Through the above steps, we can obtain the relatively accurate relation between the exerted electric field and the area strain.

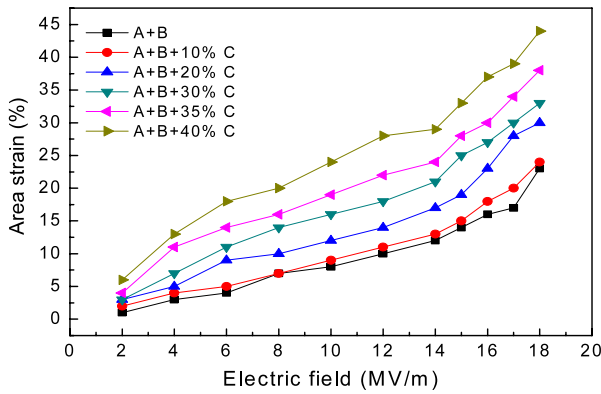


**Figure 3.** Electric field versus surface strain with different percentages of plasticizer C (pre-strain is 400%).

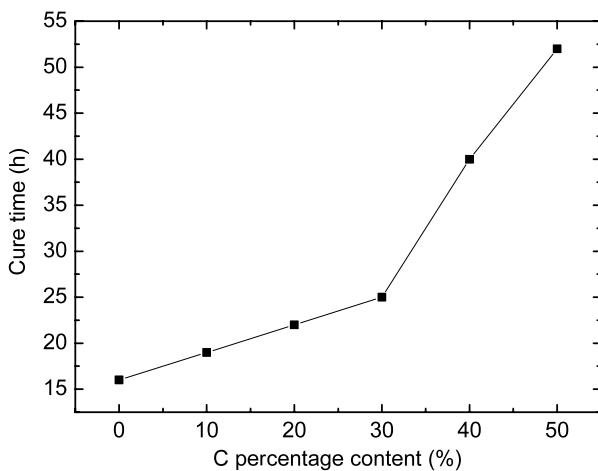


**Figure 4.** The curing time at various contents of C.

It is shown in figure 2 that the surfaces become larger with a gradually increasing applied voltage. The more the plasticizer C is present, the larger the extended surface of the actuator. This is so since the elastic modulus of the silicone film actuator reduces with the more plasticizer in it, resulting correspondingly in larger strain of the actuator.

Comparing figures 2 and 3, one can see that, as the pre-strain ratio increases, the area strain of the silicone film actuator decreases while the breakdown voltage increases. Also, the pre-strain ratio determines the rate of the area change via the variation of interior microstructures. Such changes are also responsible for the increasing rigidity of the material, i.e. the increase of the elastic modulus and the breakdown voltage.

### 3. Silicone dielectric elastomer mixed with barium titanate

A series of silicone film with different percentages of component C, A + B, A + B + 10% C, A + B + 20% C, A + B + 30% C, A + B + 40% C and A + B + 50% C, have been obtained. The different solidification times were recorded also. It is shown in figure 4 that the solidification time increases with the increase of the percentage of component C, and

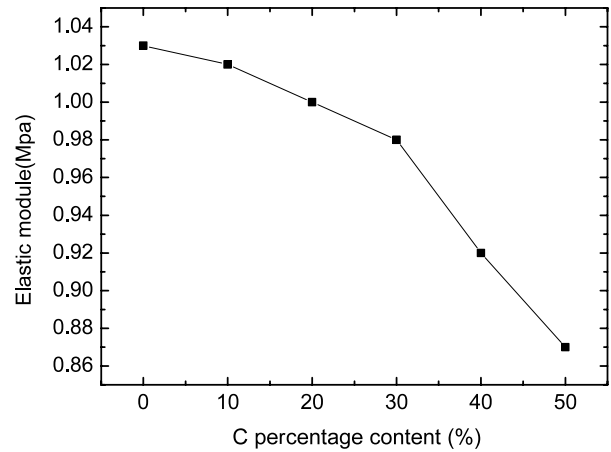


**Figure 5.** The elastic modulus at various contents of C.

the solidification time rises significantly when component C exceeds 30%, i.e. 52 h for 50% of component C. The elastic modulus of silicones with different percentages of component C are presented in figure 5, which reveals the decline of the elastic modulus when the content of C increases.

The process of fabrication of silicone filled with barium titanate is presented as follows. Component C filled with 30% silicon is selected, as the silicone shows a solidification of a short time, high modulus, and favorable elastic performance. Barium titanate is a ferroelectric relaxation material, which presents good dielectric and mechanical performance. The barium titanate was incorporated into the silicon and the composites are simplified to be expressed as follows: A + B + 30% C + 0% BaTiO<sub>3</sub>, A + B + 30% C + 1% BaTiO<sub>3</sub>, A + B + 30% C + 2% BaTiO<sub>3</sub>, A + B + 30% C + 10%. BaTiO<sub>3</sub> are stirred in a high velocity agitator, then the bubbles are removed in a vacuum chamber, injected into an aluminum model, and finally cured at room temperature.

The tests of the mechanical performance of the fabricated silicone are performed in an electronic tensile machine by using a dumbbell sample. Figure 6 gives the stress-strain curve of the silicone composite material, which implied the elastic modulus increases as the barium titanate increases and the strain of this novel material exceeds 300%. Therefore, compared with the traditional silicone, the present one is demonstrated to have a significantly enhanced elastic modulus without reducing its elastic ability.

Figures 7 and 8 represent the dielectric loss and permittivity at different percentages of barium titanate. The fact that the dielectric constant augments quickly as the percentage increases implies that the proposed silicone has more advantages than the traditional silicones in dielectric performance.

### 4. Finite element analysis of modeling the dielectric elastomer

#### 4.1. The constitutive relationship of the dielectric elastomer

Regarding the silicone-like super-elastic materials, there is an associated elastic potential energy functional in terms of the

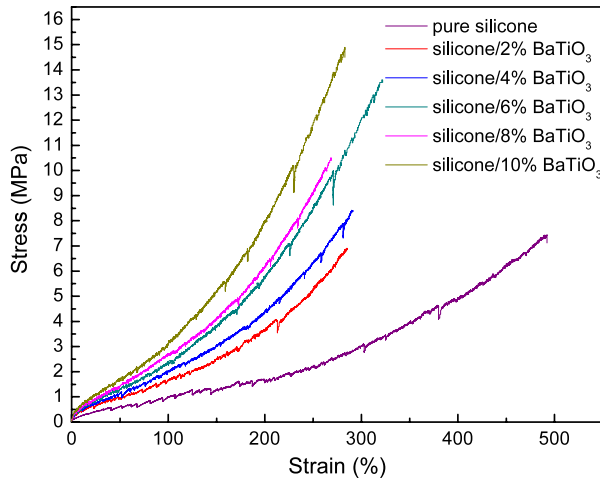


**Figure 6.** Elastic modulus at various barium titanate contents with 30%.

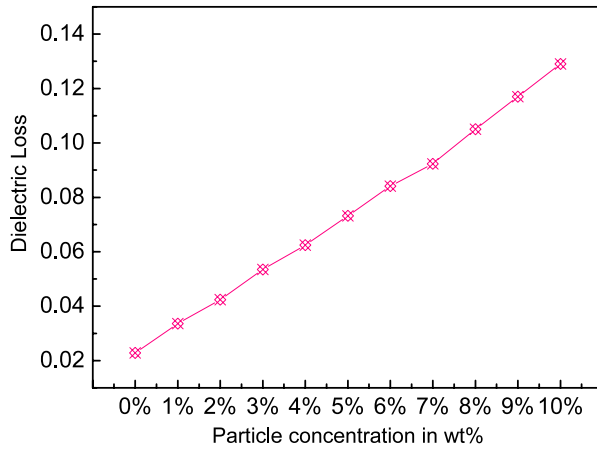


**Figure 7.** Dielectric loss of dielectric composites at varying particle concentrations.

strain invariants or the stretching invariants. Its first derivative with respect to the strain gives the corresponding second Piola–Kirchhoff stress tensor  $[S]$  [18–20], i.e.

$$[S] = \frac{\partial W}{\partial [E]} \quad (6)$$

where  $W$  is the strain energy density functional and  $[E]$  is the Lagrangian strain tensor. It is obvious that

$$[E] = \frac{1}{2}([C] - I) \quad (7)$$

where  $[C] = [F]^T[F]$  is the Cauchy–Green strain tensor and  $[I]$  denotes the identity matrix [21, 22].

The hyperelastic material is assumed to be homogeneous and isotropic, hence  $W$  can be written as an explicit function of the three strain invariants [23], i.e.

$$\begin{aligned} I_1 &= J^{-2/3}(\lambda_1^2 + \lambda_2^2 + \lambda_3^2) \\ I_2 &= J^{-2/3}(\lambda_1^2\lambda_2^2 + \lambda_3^2\lambda_2^2 + \lambda_1^2\lambda_3^2) \\ I_3 &= J^{-2/3}(\lambda_1^2\lambda_2^2\lambda_3^2) \end{aligned} \quad (8)$$

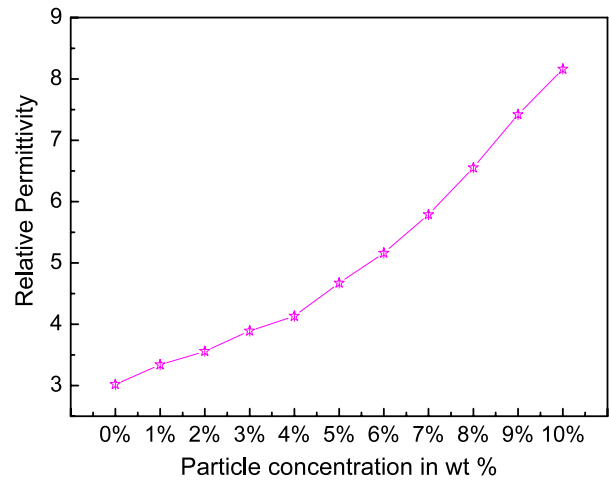


**Figure 8.** Permittivity of dielectric composites at varying particle concentrations.

where  $J$  is the ratio of initial and ultimate volume and  $\lambda_i$  ( $i = 1, 2, 3$ ) are the principal stretch ratios.

#### 4.2. Finite element analysis

In our FEA process (with ANSYS), the following two common postulates are imposed.

- (1) The silicone elastomer is treated as a hyperelastic material and the two-term Ogden model is adapted.
- (2) The silicone elastomer is incompressible.

According to the classical mathematical model for an electromechanical coupling system (equation (1)), the stress in the silicone rubber imposed by various electric fields could be calculated. For the finite element analysis, the two-term Ogden model is used here for its best approximation in the analysis of large strain which can be up to 700%. The element type is Shell-181 because of the good correspondence between the two-term Ogden model and Shell-181.

The finite element model of the silicone film actuator is depicted in figure 9. Dimensions of the element type are  $10 \times 10 \times 0.5 \text{ mm}^3$  and the element number is 100. Zero displacement and rotation angles on the four domain sides are imposed. From figure 9, it is shown that the meshes are regular and uniform. With this set-up, results from FEA simulation and experiment are compared in figure 10. It is clear that the two results match well.

In the following analysis, a different theory is applied to study the constitutive relation of the dielectric elastomers. The analytical expressions for real and nominal stress are yielded.

## 5. Hyperelastic model of dielectric elastomers

As stated above, the electroactive polymer dielectric elastomer is a super-elastic material, and assumed to be hyper-elastic [24, 25], homogeneous, isotropic and incompressible

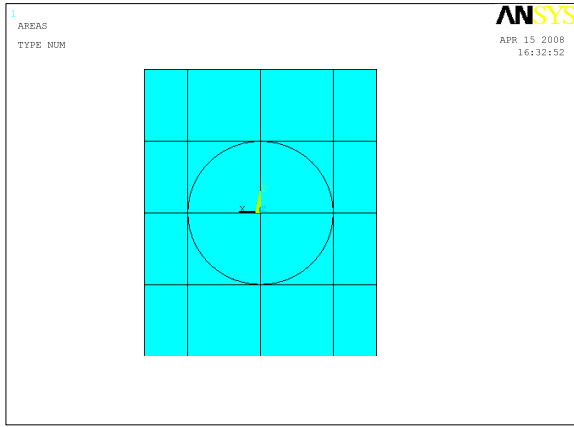


Figure 9. Finite element model of the dielectric film actuator.

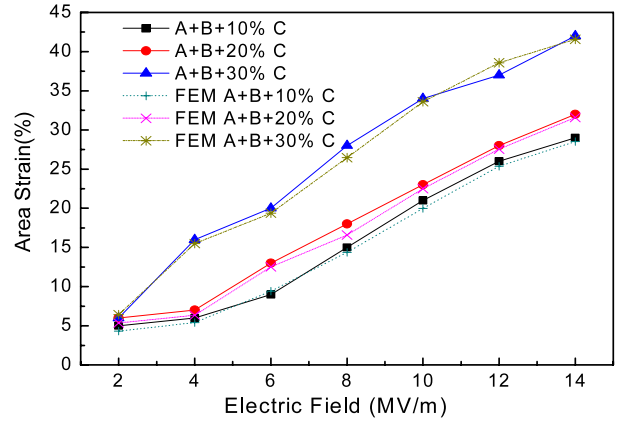


Figure 10. Comparing between finite element simulation and experimentation.

( $J = 1$ ). Then the associated elastic strain energy functional  $W$  is a function of three strain invariants:

$$I_1 = \lambda_1^2 + \lambda_2^2 + \lambda_3^2,$$

$$I_2 = \lambda_1^2\lambda_2^2 + \lambda_2^2\lambda_3^2 + \lambda_3^2\lambda_1^2 = \lambda_3^{-2} + \lambda_1^{-2} + \lambda_2^{-2},$$

$$I_3 = \lambda_1^2\lambda_2^2\lambda_3^2 = 1.$$

Taking the Ogden model, we have

$$W_0(\lambda_1, \lambda_2, \lambda_3) = \sum_{i=1}^N \frac{\mu_i}{\alpha_i} (\lambda_1^{\alpha_i} + \lambda_2^{\alpha_i} + \lambda_3^{\alpha_i} - 3) \quad (9)$$

where  $\mu_i$  and  $\alpha_i$  are the material constants. Correspondingly, the stresses are

$$\sigma_i = \lambda_i \frac{\partial W}{\partial \lambda_i} - p = \sum_{j=1}^N \mu_j \lambda_i^{\alpha_j} - p \quad (10)$$

where  $p$  is the hydrostatic pressure:  $p = \sum_{j=1}^N \mu_j \lambda_1^{-2\alpha_j}$ .

We now discuss two loading cases (figures 11 and 12). One is applying pre-strain in the film plane along directions 1 and 2; the other one is applying electrical voltage in the thickness direction (direction 3). These two cases correspond to the sub-index  $j$  ( $j = 1, 2$ ) in the notation  $\sigma_i^j$ , where  $i$  stands for the principal direction ( $i = 1, 2, 3$ ). Then for uniform stretching (loading case 1), one has

$$\sigma_1^1(\lambda) = \sigma_2^1(\lambda) = \sum_{j=1}^N \mu_j (\lambda_1^{\alpha_j} + \lambda_1^{-2\alpha_j}), \quad \sigma_3(\lambda) = 0. \quad (11)$$

Then for loading case 2, the Maxwell stresses are

$$\sigma_1^2(\lambda, u) = \sigma_2^2(\lambda, u) = \sum_{j=1}^N \mu_j (\lambda_1^{\alpha_j} + \lambda_1^{-2\alpha_j}) - \epsilon_0 \epsilon \frac{\lambda_1^4 U^2}{h_0^2} \quad (12)$$

$$\sigma_3^2(\lambda, u) = -\epsilon_0 \epsilon \frac{\lambda_1^4 U^2}{h_0^2}. \quad (13)$$

## 6. Electromechanical analysis in dielectric elastomer

As a coupled system of mechanical and electric field, the mechanical performance of the dielectric elastomer film actuator can be analyzed by the nonlinear field theory on the dielectric elastomer. For practical analysis, some basic assumptions are put forward.

- (1) The elastomer is considered as a hyperelastic material. The viscoelastic action is not taken into consideration.
- (2) The material of the electrode is an ideal liquid.
- (3) The dielectric elastomer is supposed to be an ideal dielectric.
- (4) The response of the dielectric elastomer is an isothermal process, namely the dissipation of thermal energy of the dielectric elastomer is not taken into account.

The free energy function can be decomposed as follows [26–30]:

$$W(\lambda_1, \lambda_2, \lambda_3, \tilde{D}) = W_0(\lambda_1, \lambda_2, \lambda_3) + W_1(\lambda_1, \lambda_2, \tilde{D}) \quad (14)$$

where  $\tilde{D}$  is the nominal electric displacement, and  $W_0(\lambda_1, \lambda_2, \lambda_3)$  and  $W_1(\lambda_1, \lambda_2, \tilde{D})$  are the elastic strain energy density functional and electric energy density functional, respectively. With the simplest form of Ogden model, we take

$$W_0(\lambda_1, \lambda_2, \lambda_3) = \sum_{i=1}^N \frac{\mu_i}{\alpha_i} (\lambda_1^{\alpha_i} + \lambda_2^{\alpha_i} + \lambda_3^{\alpha_i} - 3). \quad (15)$$

Under the hypothesis of satisfying the above assumptions and according to Suo's nonlinear field theory on dielectric elastomers [28],  $W_1(\tilde{D})$  is

$$W_1(\tilde{D}) = \frac{1}{2\epsilon} D_i D_i = \frac{1}{2\epsilon} D_3^2 \quad (16)$$

$$\tilde{D}_3 = \frac{Q}{A} = \frac{Q}{\lambda_3 a} = \frac{D_3}{\lambda_3} \quad (17)$$

where  $Q$  is the electric quantity that the dielectric elastomer actuator carries in the flexible electrode,  $a$  is the original area of the applied electrode on the dielectric elastomer film actuator

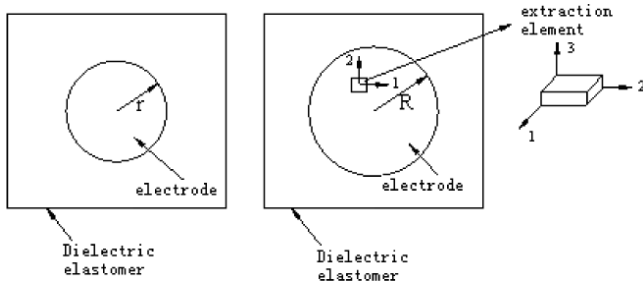


Figure 11. Schematic picture of the dielectric film actuator.

and  $A$  is the area of the applied electrode imposed by external voltage.  $D = \lambda_3 \tilde{D}$  is the true electric displacement. Note  $W_1(\tilde{D})$  is taken from literature references. The free energy function of the dielectric elastomer electromechanical coupling system can be written as:

$$W(\lambda_1, \lambda_2, \lambda_3, \tilde{D}) = \sum_{i=1}^N \frac{\mu_i}{\alpha_i} (\lambda_1^{\alpha_i} + \lambda_2^{\alpha_i} + (\lambda_1 \lambda_2)^{-\alpha_i} - 3) + \frac{1}{2\varepsilon} D^2 \quad (18)$$

$$s_{iK}(F, \tilde{D}) = \frac{\partial W(F, \tilde{D})}{\partial F_{iK}}, \quad \tilde{E}_K(F, \tilde{D}) = \frac{\partial W(F, \tilde{D})}{\partial \tilde{D}_K} \quad (19)$$

$s_{iK}(F, \tilde{D})$ ,  $\tilde{E}_K(F, \tilde{D})$  is the nominal stress and electric field of the electromechanical coupling system of the dielectric elastomer, respectively.  $F_{iK}$  is the deformation gradient tensor:

$$s_{11} = \frac{\partial W}{\partial \lambda_1} = \sum_{i=1}^N \mu_i (\lambda_1^{\alpha_i-1} - \lambda_1^{-\alpha_i-1} \lambda_2^{-\alpha_i}) \quad (20)$$

$$s_{22} = \frac{\partial W}{\partial \lambda_2} = \sum_{i=1}^N \mu_i (\lambda_2^{\alpha_i-1} - \lambda_2^{-\alpha_i-1} \lambda_1^{-\alpha_i}) \quad (21)$$

$$s_{33} = \frac{\partial W}{\partial \lambda_3} = \sum_{i=1}^N \mu_i \lambda_3^{\alpha_i-1} + \frac{\tilde{D}_3^2}{\varepsilon} \lambda_3 \quad (22)$$

$$\tilde{E}_3(F, \tilde{D}) = \frac{\partial W(F, \tilde{D})}{\partial \tilde{D}_3} = \frac{\lambda_3^2}{\varepsilon} \tilde{D}_3 = \lambda_3 E_3. \quad (23)$$

Considering the load cases of the dielectric elastomer film, the nominal stress matrix of a electromechanical coupling system is

$$s_{ij} = \begin{bmatrix} s_{11} & 0 & 0 \\ 0 & s_{22} & 0 \\ 0 & 0 & s_{33} \end{bmatrix}. \quad (24)$$

The corresponding deformation gradient matrix is

$$F_{ij} = \begin{bmatrix} \lambda_1 & 0 & 0 \\ 0 & \lambda_2 & 0 \\ 0 & 0 & \lambda_3 \end{bmatrix}. \quad (25)$$

Based on the nonlinear field theory referred, the real stress  $\sigma_{ij}$  of the electromechanical coupling system of the dielectric elastomer is

$$\sigma_{ij} = \frac{F_{jK}}{\det(F_{ij})} s_{iK} = \frac{F_{jK}}{\lambda_1 \lambda_2 \lambda_3} s_{iK} = F_{jK} s_{iK} \quad (26)$$

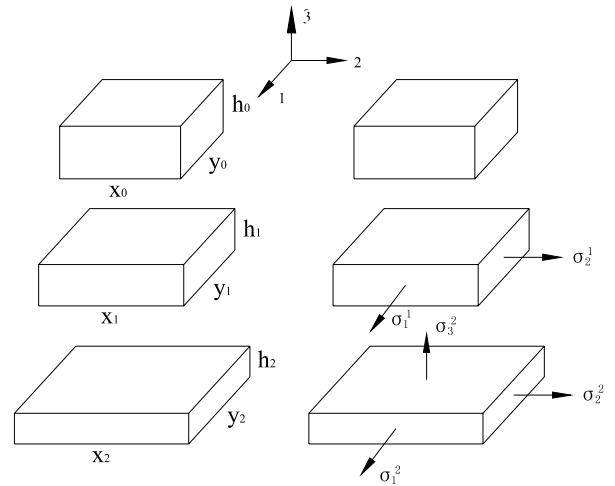


Figure 12. Mechanical analysis in different stress state.

$$\sigma_1^2 = F_{1K} s_{1K} = \sum_{i=1}^N \mu_i (\lambda_1^{\alpha_i} - \lambda_1^{-\alpha_i} \lambda_2^{-\alpha_i}) \quad (27)$$

$$\sigma_2^2 = F_{2K} s_{2K} = \sum_{i=1}^N \mu_i (\lambda_2^{\alpha_i} - \lambda_2^{-\alpha_i} \lambda_1^{-\alpha_i}) \quad (28)$$

$$\begin{aligned} \sigma_3^2 &= F_{3K} s_{3K} = \lambda_3 \left( \sum_{i=1}^N \mu_i \lambda_3^{\alpha_i-1} + \frac{\tilde{D}_3^2}{\varepsilon} \lambda_3 \right) \\ &= \sum_{i=1}^N \mu_i \lambda_3^{\alpha_i} + \varepsilon E_3^2. \end{aligned} \quad (29)$$

## 7. Electromechanical constitutive relations with variable dielectric constants

In this case, we still take

$$W_0(\lambda_1, \lambda_2, \lambda_3) = \sum_{i=1}^N \frac{\mu_i}{\alpha_i} (\lambda_1^{\alpha_i} + \lambda_2^{\alpha_i} + \lambda_3^{\alpha_i} - 3). \quad (30)$$

But a different  $W_1(\lambda_1, \lambda_2, \lambda_3, \tilde{D})$ , where

$$W_1(\lambda_1, \lambda_2, \lambda_3, \tilde{D}) = \frac{D^2}{2\varepsilon(\lambda_1, \lambda_2, \lambda_3)}. \quad (31)$$

Here,  $D = \lambda_3 \tilde{D}$ . For the variable dielectric constant  $\varepsilon(\lambda_1, \lambda_2, \lambda_3)$ , its relationship with the deformation for VHB4910 has been given by Pelrine [31] and cited in figure 13.

The figure shows clearly a transition point where the relation changes from a linearly decreasing behavior to a constant as the area increase ratio  $\lambda_1 \lambda_2$  reaches 16. An interpolation of the curves is found. We fit the expression of the dielectric constant according to the experimental data for VHB4910 obtained by Pelrine:

$$\varepsilon(\lambda_1, \lambda_2, \lambda_3) = \begin{cases} (-0.016\lambda_1\lambda_2 + 4.716)\varepsilon_0, & \lambda_1\lambda_2 \leq 16 \\ 4.48\varepsilon_0, & \lambda_1\lambda_2 \geq 16. \end{cases} \quad (32)$$

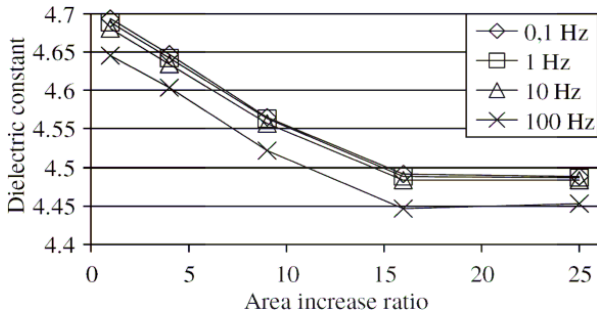


**Figure 13.** Dielectric constant versus area increase ratio of VHB 4910.

For generality and representativity, the dielectric constant of the dielectric elastomer can be expressed as follows:

$$\varepsilon(\lambda_1, \lambda_2, \lambda_3) = \begin{cases} (c_1\lambda_1\lambda_2 + c_2)\varepsilon_0, & \lambda_1\lambda_2 \leq a \\ c_3\varepsilon_0, & \lambda_1\lambda_2 \geq a. \end{cases} \quad (33)$$

Here  $c_1, c_2, c_3, a$  are constants. For acrylic VHB4910,  $c_1 = -0.016, c_2 = 4.716, c_3 = 4.48, a = 16$ .

When  $\lambda_1\lambda_2 \leq a$ , by incompressibility,  $\lambda_3 = 1/\lambda_1\lambda_2$ . The electric energy density function and free energy function of the dielectric elastomer can be expressed as follows:

$$W_1(\lambda_1, \lambda_2, \tilde{D}) = \frac{\tilde{D}^2}{2\varepsilon_0(c_1\lambda_1\lambda_2 + c_2)}\lambda_1^{-2}\lambda_2^{-2} \quad (34)$$

$$W_0(\lambda_1, \lambda_2, \lambda_3) = \sum_{i=1}^N \frac{\mu_i}{\alpha_i} (\lambda_1^{\alpha_i} + \lambda_2^{\alpha_i} + \lambda_3^{\alpha_i} - 3). \quad (35)$$

When the shear deformation and nominal stress are ignored, the electric field strength can be derived from equation (19), where

$$s_{11} = \frac{\partial W}{\partial \lambda_1} = \sum_{i=1}^N \mu_i (\lambda_1^{\alpha_i-1} - \lambda_1^{-\alpha_i-1} \lambda_2^{-\alpha_i}) - \frac{\tilde{D}^2}{2\varepsilon_0} \frac{3c_1\lambda_1^{-2}\lambda_2^{-1} + 2c_2\lambda_1^{-3}\lambda_2^{-2}}{(c_1\lambda_1\lambda_2 + c_2)^2} \quad (36)$$

$$s_{22} = \frac{\partial W}{\partial \lambda_2} = \sum_{i=1}^N \mu_i (\lambda_2^{\alpha_i-1} - \lambda_2^{-\alpha_i-1} \lambda_1^{-\alpha_i}) - \frac{\tilde{D}^2}{2\varepsilon_0} \frac{3c_1\lambda_1^{-1}\lambda_2^{-2} + 2c_2\lambda_1^{-2}\lambda_2^{-3}}{(c_1\lambda_1\lambda_2 + c_2)^2} \quad (37)$$

$$s_{33} = \frac{\partial W}{\partial \lambda_3} = \sum_{i=1}^N \mu_i \lambda_3^{\alpha_i-1} + \frac{\tilde{D}^2}{\varepsilon_0(c_1\lambda_1\lambda_2 + c_2)} \lambda_3 \quad (38)$$

$$\tilde{E} = \frac{\partial W}{\partial \tilde{D}} = \frac{\tilde{D}}{\varepsilon_0(c_1\lambda_1\lambda_2 + c_2)} \lambda_1^{-2}\lambda_2^{-2}. \quad (39)$$

All other components are zero.

Combining equation (26), the true stresses and the true electric field can be found [27] to be

$$\sigma_{ij} = \frac{F_{jK}}{\det(F_{ij})} s_{iK} = \frac{F_{jK}}{\lambda_1\lambda_2\lambda_3} s_{iK} = F_{jK} s_{iK} \quad (40)$$

$$\sigma_1^2 = F_{1K} s_{1K} = \lambda_1 s_{11} = \sum_{i=1}^N \mu_i (\lambda_1^{\alpha_i} - \lambda_1^{-\alpha_i} \lambda_2^{-\alpha_i})$$

$$- \frac{\tilde{D}^2}{2\varepsilon_0} \frac{3c_1\lambda_1^{-1}\lambda_2^{-1} + 2c_2\lambda_1^{-2}\lambda_2^{-2}}{(c_1\lambda_1\lambda_2 + c_2)^2} \quad (41)$$

$$\sigma_2^2 = F_{2K} s_{2K} = \lambda_2 s_{22} = \sum_{i=1}^N \mu_i (\lambda_2^{\alpha_i} - \lambda_2^{-\alpha_i} \lambda_1^{-\alpha_i}) - \frac{\tilde{D}^2}{2\varepsilon_0} \frac{3c_1\lambda_1^{-1}\lambda_2^{-1} + 2c_2\lambda_1^{-2}\lambda_2^{-2}}{(c_1\lambda_1\lambda_2 + c_2)^2} \quad (42)$$

$$\sigma_3^2 = F_{3K} s_{3K} = \lambda_3 s_{33} = \sum_{i=1}^N \mu_i \lambda_3^{\alpha_i} + \frac{\tilde{D}^2}{\varepsilon_0(c_1\lambda_1\lambda_2 + c_2)} \lambda_3^2. \quad (43)$$

When  $\lambda_1\lambda_2 > a$ , the electric energy density function and free energy function of the dielectric elastomer can be expressed as follows:

$$W_1(\lambda_1, \lambda_2, \tilde{D}) = \frac{\tilde{D}^2}{2c_3\lambda_1^2\lambda_2^2\varepsilon_0} \quad (44)$$

$$W(\lambda_1, \lambda_2, \lambda_3, D) = \sum_{i=1}^N \frac{\mu_i}{\alpha_i} (\lambda_1^{\alpha_i} + \lambda_2^{\alpha_i} + (\lambda_1\lambda_2)^{-\alpha_i} - 3) + \frac{\tilde{D}^2}{2c_3\lambda_1^2\lambda_2^2\varepsilon_0}. \quad (45)$$

Substituting equation (44) into equation (18), the nominal stress and the nominal electric field can be expressed respectively as follows:

$$s_{11} = \frac{\partial W}{\partial \lambda_1} = \sum_{i=1}^N \mu_i (\lambda_1^{\alpha_i-1} - \lambda_1^{-\alpha_i-1} \lambda_2^{-\alpha_i}) - \frac{\tilde{D}^2}{c_3\varepsilon_0} \lambda_1^{-3}\lambda_2^{-2} \quad (46)$$

$$s_{22} = \frac{\partial W}{\partial \lambda_2} = \sum_{i=1}^N \mu_i (\lambda_2^{\alpha_i-1} - \lambda_2^{-\alpha_i-1} \lambda_1^{-\alpha_i}) - \frac{\tilde{D}^2}{c_3\varepsilon_0} \lambda_1^{-2}\lambda_2^{-3} \quad (47)$$

$$s_{33} = \frac{\partial W}{\partial \lambda_3} = \sum_{i=1}^N \mu_i \lambda_3^{\alpha_i-1} + \frac{\tilde{D}^2}{c_3\varepsilon_0} \lambda_3 \quad (48)$$

$$\tilde{E} = \frac{\partial W}{\partial \tilde{D}} = \frac{\tilde{D}}{c_3\varepsilon_0} \lambda_1^{-2}\lambda_2^{-2}. \quad (49)$$

Consider the relation between the true and the nominal stress. Expression of the true stress can be derived:

$$\sigma_1^2 = F_{1K} s_{1K} = \lambda_1 s_{11} = \sum_{i=1}^N \mu_i (\lambda_1^{\alpha_i} - \lambda_1^{-\alpha_i} \lambda_2^{-\alpha_i}) - \frac{\tilde{D}^2}{c_3\varepsilon_0} \lambda_1^{-2}\lambda_2^{-2} \quad (50)$$

$$\sigma_2^2 = F_{2K} s_{2K} = \lambda_2 s_{22} = \sum_{i=1}^N \mu_i (\lambda_2^{\alpha_i} - \lambda_2^{-\alpha_i} \lambda_1^{-\alpha_i}) - \frac{\tilde{D}^2}{c_3\varepsilon_0} \lambda_1^{-2}\lambda_2^{-2} \quad (51)$$

$$\sigma_3^2 = F_{3K} s_{3K} = \lambda_3 s_{33} = \sum_{i=1}^N \mu_i \lambda_3^{\alpha_i} + \frac{\tilde{D}^2}{c_3\varepsilon_0} \lambda_3^2. \quad (52)$$

## 8. Dielectric elastomer undergoing free deformation

In sections 5–7, we establish the constitutive relation of the dielectric elastomer based on the assumption of incompressibility. The incompressibility is regarded as a constraint condition, namely the deformation is not arbitrary. In this section we establish the constitutive relation of the dielectric elastomer undergoing free deformation imposed by electromechanical excitation.

Introducing the Lagrange multiplier  $p$ , we modify the Ogden hyperelastic strain energy function  $W_0(\lambda_1, \lambda_2, \lambda_3)$  to

$$W'_0(\lambda_1, \lambda_2, \lambda_3) = \sum_{i=1}^N \frac{\mu_i}{\alpha_i} (\lambda_1^{\alpha_i} + \lambda_2^{\alpha_i} + \lambda_3^{\alpha_i} - 3) - p(\lambda_1 \lambda_2 \lambda_3 - 1). \quad (53)$$

When the dielectric elastomer undergoes free deformation,  $\lambda_1 \lambda_2 \lambda_3 \neq 1$ . Substitute equations (16) and (17) into (19) and (26). Similar to the above, the expression of the nominal and real stress in the dielectric elastomer can be yielded from the electric field energy density function with invariable dielectric constant:

$$s_{11} = \frac{\partial W}{\partial \lambda_1} = \sum_{i=1}^N \mu_i (\lambda_1^{\alpha_i - 1} - \lambda_1^{-\alpha_i - 1} \lambda_2^{-\alpha_i}) - p \lambda_1^{-1} \quad (54)$$

$$s_{22} = \frac{\partial W}{\partial \lambda_2} = \sum_{i=1}^N \mu_i (\lambda_2^{\alpha_i - 1} - \lambda_2^{-\alpha_i - 1} \lambda_1^{-\alpha_i}) - p \lambda_2^{-1} \quad (55)$$

$$s_{33} = \frac{\partial W}{\partial \lambda_3} = \sum_{i=1}^N \mu_i \lambda_3^{\alpha_i - 1} - p \lambda_3^{-1} + \frac{\tilde{D}_3^2}{\varepsilon} \lambda_3 \quad (56)$$

$$\sigma_1^2 = F_{1K} s_{1K} = \sum_{i=1}^N \mu_i (\lambda_1^{\alpha_i} - \lambda_1^{-\alpha_i} \lambda_2^{-\alpha_i}) - p \quad (57)$$

$$\sigma_2^2 = F_{2K} s_{2K} = \sum_{i=1}^N \mu_i (\lambda_2^{\alpha_i} - \lambda_2^{-\alpha_i} \lambda_1^{-\alpha_i}) - p \quad (58)$$

$$\begin{aligned} \sigma_3^2 &= F_{3K} s_{3K} = \lambda_3 \left( \sum_{i=1}^N \mu_i \lambda_3^{\alpha_i - 1} - p \lambda_3^{-1} + \frac{\tilde{D}_3^2}{\varepsilon} \lambda_3 \right) \\ &= \sum_{i=1}^N \mu_i \lambda_3^{\alpha_i} - p + \varepsilon E_3^2. \end{aligned} \quad (59)$$

In terms of (34), (53), (19) and (26), we obtain the formulation of the real stress in the dielectric elastomer by use of an electric field energy density function (when  $\lambda_1 \lambda_2 \leq a$ ) with variational dielectric constant

$$\begin{aligned} \sigma_1^2 &= \sum_{i=1}^N \mu_i (\lambda_1^{\alpha_i} - \lambda_1^{-\alpha_i} \lambda_2^{-\alpha_i}) - p \\ &\quad - \frac{\tilde{D}^2}{2\varepsilon_0} \frac{3c_1 \lambda_1^{-1} \lambda_2^{-1} + 2c_2 \lambda_1^{-2} \lambda_2^{-2}}{(c_1 \lambda_1 \lambda_2 + c_2)^2} \end{aligned} \quad (60)$$

$$\begin{aligned} \sigma_2^2 &= \sum_{i=1}^N \mu_i (\lambda_2^{\alpha_i} - \lambda_2^{-\alpha_i} \lambda_1^{-\alpha_i}) - p \\ &\quad - \frac{\tilde{D}^2}{2\varepsilon_0} \frac{3c_1 \lambda_1^{-1} \lambda_2^{-1} + 2c_2 \lambda_1^{-2} \lambda_2^{-2}}{(c_1 \lambda_1 \lambda_2 + c_2)^2} \end{aligned} \quad (61)$$

$$\sigma_3^2 = \sum_{i=1}^N \mu_i \lambda_3^{\alpha_i} - p + \frac{\tilde{D}^2}{\varepsilon_0 (c_1 \lambda_1 \lambda_2 + c_2)} \lambda_3^2. \quad (62)$$

Considering equations (44), (53), (19) and (26), the real stress of the electromechanical coupling system is obtained when  $\lambda_1 \lambda_2 > a$ :

$$\sigma_1^2 = \sum_{i=1}^N \mu_i (\lambda_1^{\alpha_i} - \lambda_1^{-\alpha_i} \lambda_2^{-\alpha_i}) - p - \frac{\tilde{D}^2}{c_3 \varepsilon_0} \lambda_1^{-2} \lambda_2^{-2} \quad (63)$$

$$\sigma_2^2 = \sum_{i=1}^N \mu_i (\lambda_2^{\alpha_i} - \lambda_2^{-\alpha_i} \lambda_1^{-\alpha_i}) - p - \frac{\tilde{D}^2}{c_3 \varepsilon_0} \lambda_1^{-2} \lambda_2^{-2} \quad (64)$$

$$\sigma_3^2 = \sum_{i=1}^N \mu_i \lambda_3^{\alpha_i} - p + \frac{\tilde{D}^2}{c_3 \varepsilon_0} \lambda_3^2. \quad (65)$$

## 9. Constitutive law of novel silicone dielectric elastomer

It is shown in figure 6 that the solidification time increases as the increase of the percentage of component C and the solidification time rises significantly when component C exceeds 30%, i.e. 52 h for 50% of component C. It demonstrates that, compared with the pure silicone, the silicone filled with barium titanate has better mechanical performances (elastic modulus, driving force, etc), but does not lose the silicone's excellent hyperelastic. To describe the elasticity of this new type of silicone, a developed Ogden model is given as follows:

$$W_0(\lambda_1, \lambda_2, \lambda_3, v) = \sum_{i=1}^N \frac{\mu_i(v)}{\alpha_i} (\lambda_1^{\alpha_i} + \lambda_2^{\alpha_i} + \lambda_3^{\alpha_i} - 3) \quad (66)$$

where  $\mu_i(v)$  are the material constants which depend on the percentage of component C. According to the experimental data, the dielectric constant can be expressed as follows:

$$\varepsilon(v) = \varepsilon'_0 + c(v)\varepsilon'_0 \quad (67)$$

where  $\varepsilon'_0$  is the dielectric constant at  $C\% = 30\%$  and  $c(v)$  is a coefficient depending on the percentage of barium titanate. We make a linearization of  $c(v)$ :

$$c(v) = a + bv \quad (68)$$

where  $a$  and  $b$  are the constants related to the percentage of barium titanate. When  $c(1\%) = 0.106$ ,  $c(4\%) = 0.365$ , then  $a = 0.02$ ,  $b = 8.6$ ; if  $c(5\%) = 0.546$ ,  $c(10\%) = 1.701$ , then  $a = -0.609$ ,  $b = 23.1$ .  $C(v)$  can be expressed as an fractional function:

$$c(v) = \begin{cases} 0.02 + 8.6v, & 0 \leq v \leq 0.04 \\ -0.609 + 23.1v, & 0.04 < v \leq 0.1. \end{cases} \quad (69)$$

Considering the mathematical expression of the free energy of the dielectric silicone-based electromechanical coupling system:

$$\begin{aligned} W(\lambda_1, \lambda_2, \lambda_3, v, \tilde{D}) &= \sum_{i=1}^N \frac{\mu_i(v)}{\alpha_i} (\lambda_1^{\alpha_i} + \lambda_2^{\alpha_i} + \lambda_3^{\alpha_i} - 3) \\ &\quad + \frac{\tilde{D}^2}{2(1 + a + bv)\varepsilon'_0} \lambda_1^{-2} \lambda_2^{-2}. \end{aligned} \quad (70)$$



The nominal stresses of the silicone composite material are expressed as follows;

$$s_{11} = \sum_{i=1}^N \mu_i(v)(\lambda_1^{\alpha_i-1} - \lambda_1^{-\alpha_i-1}\lambda_2^{-\alpha_i}) - \frac{\tilde{D}^2}{(1+a+bv)\varepsilon'_0}\lambda_1^{-3}\lambda_2^{-2} \quad (71)$$

$$s_{22} = \sum_{i=1}^N \mu_i(v)(\lambda_2^{\alpha_i-1} - \lambda_2^{-\alpha_i-1}\lambda_1^{-\alpha_i}) - \frac{\tilde{D}^2}{(1+a+bv)\varepsilon'_0}\lambda_1^{-2}\lambda_2^{-3} \quad (72)$$

$$s_{33} = \sum_{i=1}^N \mu_i(v)\lambda_3^{\alpha_i-1} + \frac{\tilde{D}^2}{(1+a+bv)\varepsilon'_0}\lambda_3. \quad (73)$$

Correspondingly, the true stress is

$$\sigma_1^2 = \sum_{i=1}^N \mu_i(v)(\lambda_1^{\alpha_i} - \lambda_1^{-\alpha_i}\lambda_2^{-\alpha_i}) - \frac{\tilde{D}^2}{(1+a+bv)\varepsilon'_0}\lambda_1^{-2}\lambda_2^{-2} \quad (74)$$

$$\sigma_2^2 = \sum_{i=1}^N \mu_i(v)(\lambda_2^{\alpha_i} - \lambda_2^{-\alpha_i}\lambda_1^{-\alpha_i}) - \frac{\tilde{D}^2}{(1+a+bv)\varepsilon'_0}\lambda_1^{-2}\lambda_2^{-2} \quad (75)$$

$$\sigma_3^2 = \sum_{i=1}^N \mu_i(v)\lambda_3^{\alpha_i} - \frac{\tilde{D}^2}{(1+a+bv)\varepsilon'_0}\lambda_3^2. \quad (76)$$

Based on the study of sections 7 and 8, when both the constraint deformation and free deformation are considered, the true stress at free deformation can be given:

$$\sigma_1^2 = \sum_{i=1}^N \mu_i(v)(\lambda_1^{\alpha_i} - \lambda_1^{-\alpha_i}\lambda_2^{-\alpha_i}) - p - \frac{\tilde{D}^2}{(1+a+bv)\varepsilon'_0}\lambda_1^{-2}\lambda_2^{-2} \quad (77)$$

$$\sigma_2^2 = \sum_{i=1}^N \mu_i(v)(\lambda_2^{\alpha_i} - \lambda_2^{-\alpha_i}\lambda_1^{-\alpha_i}) - p - \frac{\tilde{D}^2}{(1+a+bv)\varepsilon'_0}\lambda_1^{-2}\lambda_2^{-2} \quad (78)$$

$$\sigma_3^2 = \sum_{i=1}^N \mu_i(v)\lambda_3^{\alpha_i} - p - \frac{\tilde{D}^2}{(1+a+bv)\varepsilon'_0}\lambda_3^2. \quad (79)$$

Summarizing sections 6–9, we derived the constitutive relation of the traditional and new types of dielectric elastomer under the condition of free deformation and deformation under restraint. Equations (27)–(29) are the stress–strain relation of the ideal dielectric elastomer under the condition of restrained deformation, derived by applying the Ogden elastic strain energy function and the invariable dielectric constant of the electric field energy density function. Equations (41)–(43) and (50)–(52) give the stress–strain relationship of the ideal dielectric elastomer under the condition of restrained deformation and free deformation, both of which are derived by applying the Ogden elastic strain energy function and nonlinear dielectric constant of the electric field energy density function. Equations (74)–(76) and (77)–(79) present the

constitutive relation of the new dielectric elastomer under the condition of restrained deformation and free deformation, both of which are derived by applying the developed Ogden elastic strain energy function of the dielectric constant and linear changes in the electric field energy density function.

## 10. Conclusion

In this paper, fabrication of a silicone film actuator is presented. Its deformation behavior is then studied both experimentally and numerically by finite element analysis. Experimental results show that the pre-strain ratio greatly affects the performance of the actuator. A larger pre-strain ratio leads to higher breakdown voltage and area strain. These findings are supported by the numerical simulations on three kinds of actuators. Another factor affecting the change of the area of the silicone film actuator is the content percentage of the plasticizer. When the plasticizer in the material becomes greater, the elastomer becomes softer and the solidification is longer, which degrades the performance of the actuator. The barium titanate with high permittivity was added to the raw silicone to fabricate a new dielectric elastomer. The experimental results showed that the elastomer modulus and permittivity were significantly improved.

Also, the nonlinear field theory of deformable dielectrics and hyperelastic theory are used to analyze the electromechanical field appearing in these actuators. An applied elastic strain energy function is obtained from the representative Ogden model. The electric energy function involves invariant and variable dielectric constant, respectively. Then we deduce the constitutive relation for the dielectric elastomer film actuator based on the selected function. Furthermore the mechanical behavior of the dielectric elastomer undergoing large free deformation is studied. The constitutive modulus of the dielectric elastomer composite under free deformation and restrained deformation is derived. Finally the Ogden model was developed to characterize the elastic behavior of the new dielectric elastomer. The constitutive modulus of the dielectric elastomer composite under free deformation and restrained deformation is derived. This is a promising analysis method for the study of coupled fields and mechanical properties of the dielectric film actuator.

## References

- [1] Pelrine R, Kornbluh R, Pei Q B and Joseph J 2000 *Science* **287** 836
- [2] Smela E, Inganäs O and Lundström I 1995 *Science* **268** 1735
- [3] Pelrine R E, Kornbluh R D and Joseph J P 1998 *Sensors Actuators A* **64** 77
- [4] Plante J S and Dubowsky S 2007 *Smart Mater. Struct.* **16** S227
- [5] Wissler M and Mazza E 2007 *Sensors Actuators A* **120** 185
- [6] Kofod G, Paajanen M and Bauer S 2006 *Appl. Phys. A* **85** 141
- [7] Liu L W, Fan J M, Zhang Z, Shi L, Liu Y J and Leng J S 2008 *Adv. Mater. Res.* **47–50** 298–301
- [8] Carpi F and Rossi D De 2005 *IEEE Trans. Dielectr. Electr. Insul.* **12** 835
- [9] Zhang X Q, Lowe C, Wissler M, Jahne B and Kovacs G 2005 *Adv. Eng. Mater.* **7** 361
- [10] Zhang Z, Liu L W, Fan J M, Yu K, Liu Y J, Shi L and Leng J S 2008 *Proc. SPIE* **6926** 692610

- [11] Su J, Xu T B, Zhang S J, ShROUT T R and Zhang Q M 2004 *Appl. Phys. Lett.* **85** 1045
- [12] Liu Y J, Shi L, Liu L W, Zhang Z and Leng J S 2008 *Proc. SPIE* **6927** 69271A
- [13] Kofod G, Sommer-Larsen P, Kronbluh R, Pelrine R and Intell J 2000 *Mater. Syst. Struct.* **14** 787
- [14] Zhang Z, Liu L W, Deng G, Sun S H and Leng J S 2008 *Proc. SPIE* **7287** 72871V
- [15] Liu L W, Liu Y J, Zhang Z, Yu K, Deng G, Sun S H, Shi L and Leng J S 2009 *Proc. SPIE* **7287** 728719(1)
- [16] Patrick L, Gabor K and Silvain M 2007 *Sensors Actuators A* **135** 748
- [17] Wissler M and Mazza E 2007 *Sensors Actuators A* **134** 494
- [18] Liu Y J, Liu L W, Sun S H, Shi L and Leng J S 2009 *Appl. Phys. Lett.* **94** 096101
- [19] Leng J S, Liu L W, Liu Y J, Yu K and Sun S H 2009 *Appl. Phys. Lett.* **94** 211901
- [20] Goulbourne N C, Mockensturm E M and Frecker M I 2007 *Int. J. Solids Struct.* **44** 2609
- [21] Arruda E M and Boyce M C 1993 *J. Mech. Phys. Solids* **41** 389
- [22] Chater E and Hutchinson J W 1984 *J. Appl. Mech.* **51** 269
- [23] Corona E and Kyriakides S 1998 *Int. J. Solids Struct.* **24** 505
- [24] Norris A N 2007 *Appl. Phys. Lett.* **92** 026101
- [25] Kofoda G, Wirges W, Paajanen M and Bauer S 2007 *Appl. Phys. Lett.* **90** 081916
- [26] Zhao X and Suo Z 2007 *Appl. Phys. Lett.* **91** 061921
- [27] Zhao X, Hong W and Suo Z 2007 *Phys. Rev. B* **76** 134113
- [28] Suo Z, Zhao X and Greene W H 2008 *J. Mech. Phys. Solids* **56** 476
- [29] Zhou J, Hong W, Zhao X, Zhang Z and Suo Z 2008 *J. Solids Struct.* **45** 3739
- [30] Liu Y, Liu L, Zhang Z, Shi L and Leng J 2008 *Appl. Phys. Lett.* **93** 106101
- [31] Kofod G, Sommer-Larsen P, Kronbluh R and Pelrine R 2003 *J. Intell. Mater. Syst. Struct.* **14** 787